Published in "The Journal of Physical Chemistry A 114(3): 1474–1484, 2010"
which should be cited to refer to this work.

Low-Energy Electron Attachment to the Dichlorodifluoromethane (CCl_2F_2) Molecule†

K. Graupner,‡ S. A. Haughey,‡ T. A. Field,‡ C. A. Mayhew,‡,§ T. H. Hoffmann,∥,⊥ O. May,∥ J. Fedor,∥ M. Allan,∥ I. I. Fabrikant,# E. Illenberger,▽ M. Braun,⊥ M.-W. Ruf,⊥ and H. Hotop*,⊥

Department of Physics and Astronomy, Queen's University, Belfast BT7 1NN, U.K., School of Physics and Astronomy, University of Birmingham, Birmingham B15 2TT, U.K., Département de Chimie, Université de Fribourg, CH-1700 Fribourg, Switzerland, Fachbereich Physik, Technische Universität Kaiserslautern, 67653 Kaiserslautern, Germany, Department of Physics and Astronomy, University of Nebraska, Lincoln, Nebraska 68588, and Physikalische und Theoretische Chemie, Freie Universität Berlin, 14195 Berlin, Germany

Results from a joint experimental study of electron attachment to dichlorodifluoromethane (CCl_2F_2) molecules in the gas phase are reported. In a high resolution electron beam experiment involving two versions of the laser photoelectron attachment method, the relative cross section for formation of the dominant anion Cl^- was measured over the energy range 0.001−1.8 eV at the gas temperature $T_G = 300$ K. It exhibits cusp structure at thresholds for vibrational excitation of the $\nu_3(a_1)$ mode due to interaction with the attachment channels. With reference to the thermal attachment rate coefficient $k(T = 300\ K) = 2.2(8) \times 10^{-9}\ cm^3\ s^{-1}$ (fitted average from several data), a new highly resolved absolute attachment cross section for $T_G = 300$ K was determined. Partial cross sections for formation of the anions Cl^-, Cl_2^-, F^-, ClF^-, and CCl_2F^- were measured over the range 0−12 eV, using three different electron beam experiments of medium energy resolution. The dependence of the attachment rate coefficient $k(T_e;T_G = 300\ K)$ on electron temperature T_e was calculated over the range 50−15 000 K, based on a newly constructed total cross section for anion formation at $T_G = 300$ K. R-matrix calculations for Cl^- production have been carried out for comparison with the experimental data. The R-matrix results are in line with the main experimental observations and predict the dependence of the DEA cross section on the initial vibrational level ν_3 and on the vibrational temperature. Furthermore, the cross section for vibrational excitation of the ν_3 mode has been computed.

I. Introduction

Attachment of low-energy electrons to molecules is an important process in gaseous dielectrics and other environments including excimer lasers, discharges used for etching, and the earth's atmosphere.[1−3] Because of the high electron affinity of halogen atoms Y dissociative electron attachment (DEA) to halogen-containing molecules XY (short notation Y^-/XY)

$$e^-(E) + XY \rightarrow XY^-{}^*(TNI) \rightarrow X + Y^- \qquad (1)$$

may often occur with large cross sections $\sigma(E)$ down to zero electron energy E, thus efficiently producing halogen anions as well as halogen atoms or halogen containing radicals which are important precursors for further reactions.[1−5] Following its formation, the excited, temporary negative ion $XY^-{}^*$ (TNI) can either decay by autodetachment (corresponding to elastic or inelastic electron scattering) or it may dissociate, thereby forming stable negative ions Y^-.

One point of special interest in studies of the DEA process is the relation between the resonance energy (vertical attachment energy (VAE)) and the size of the thermal attachment rate coefficient as well as the DEA cross section at its respective maximum, and the variation of these quantities with chemical substitution.[6−9] For the case of the chlorofluoromethane molecules CCl_4, CCl_3F, CCl_2F_2, and $CClF_3$, the lowest TNI state of these molecules has $^2A_1$ symmetry; it is responsible for electron attachment to these molecules at low energies via the process ($q = 0−3$, $p + q = 4$)

$$e^- + CCl_pF_q \rightarrow CCl_pF_q^-{}^*(^2A_1) \rightarrow CCl_{p-1}F_q + Cl^- \qquad (2)$$

The VAE of these molecules was determined by electron transmission spectroscopy (ETS).[8,10,11] For CCl_4, the $^2A_1$ anion state has a negative VAE (from −0.34 to −0.08 eV[6,9]), that is, it is bound relative to the vibrationless neutral molecule in the equilibrium conformation; its presence close to zero energy induces a very large attachment cross section at low energies, resulting in a high thermal attachment rate coefficient of $k(300\ K) = 3.79(19) \times 10^{-7}\ cm^3\ s^{-1}$.[12] Substituting Cl atoms with F atoms raises the VAE substantially from 0.47 eV for CCl_3F to 1.83 eV for $CClF_3$[8] while the thermal (300 K) attachment rate coefficients for these three molecules, relative to that for CCl_4, drop by factors of about 2, 10^2, and 10^6, respectively.[13] Note that the DEA reaction 2 is an exothermic process for CCl_4, CCl_3F, and CCl_2F_2 since the electron affinity of Cl (3.6127 eV[14]) exceeds the respective dissociation energy (D^0_{298K} = 3.07, 3.33(9), 3.46(11) eV) for these three molecules;[15] for $CClF_3$ (D^0_{298K} = 3.784(39) eV[15]) reaction 2 is slightly endothermic.

* To whom correspondence should be addressed. E-mail: hotop@physik.uni-kl.de.
‡ Queen's University.
§ University of Birmingham.
∥ Université de Fribourg.
⊥ Technische Universität Kaiserslautern.
University of Nebraska.
▽ Freie Universität Berlin.

The variation of the respective rate coefficients reflects the fact that electron attachment to molecules in the vibrational ground state at low electron energies is efficient only if the anion potential surface crosses that of the neutral near the equilibrium distance of the reaction coordinate, as is the case for CCl_4 and, somewhat less favorably, for CCl_3F. When the anion curve is raised to higher energies by increasing the VAE, its crossing point with the neutral curve is raised to larger distances and the Franck−Condon factor for attachment of near-zero energy electrons to molecules in the vibrational ground state decreases exponentially. In these cases, including CCl_2F_2[16] and $CClF_3$,[17,18] attachment to vibrationally excited molecules will exhibit strongly enhanced attachment cross sections at low electron energies.[19] Correspondingly, the vibrationally averaged cross section and the rate coefficient will show an Arrhenius-type rise with increasing vibrational temperature.[19−21]

For the molecules CCl_4[22,23] and CCl_3F,[24] which have large near-zero energy cross sections with negligible or weak temperature variation, high resolution attachment cross sections (energy widths down to about 0.5 meV) have been recently measured with the laser photoelectron attachment (LPA) method and joined[22,24] with electron beam data (energy width around 0.08 eV)[8] toward higher energies. Dichlorodifluoromethane CCl_2F_2 is the subject of the present article while such data are not yet available for $CClF_3$.

The importance of the molecule CCl_2F_2 for applications has been discussed in refs 3 and 16. It has a particular history as in earlier times (until about three decades ago) CCl_2F_2 was extensively used as a refrigerant and propellant. This was based on its remarkable chemical and photochemical stability and its very appropriate vaporisation temperature (243 K). On the other hand, because of its inertness CF_2Cl_2 released into the atmosphere is gradually transported as an intact molecule into the stratosphere where absorption by UV photons (at energies larger than 5.5 eV) induces the release of Cl radicals. These radicals in turn are involved in a catalytic cycle decomposing ozone.[25]

In the following we concentrate on the properties of the CCl_2F_2 molecule relevant for dissociative electron attachment. It possesses an electric dipole moment of 0.51(5) Debye = 0.20(2) au[15] and a dipole polarizability of 53.5 a_0^3 (a_0 = Bohr radius = 52.9177 pm),[15] leading to a substantial long-range attraction for the electron. Electron collisions with CCl_2F_2 at low energies are strongly influenced by four negative ion resonances,[8,10,16] in which the added electron resides in orbitals labeled as[10] a_1(C−Cl σ^*) (VAE = 0.97 eV[8]), b_2(C−Cl σ^*) (VAE = 2.36 eV[8]), a_1(C−F σ^*) (VAE = 3.86 eV[8]), and b_1(C−F σ^*) (VAE = 6.2 eV[16]). These resonances show up in total scattering,[11,16,26−29] vibrational excitation (VE),[30] electronic excitation,[16] and attachment cross sections.[8,16,31−39] Studies of VE revealed a strong mode selectivity of the resonances;[30] energy loss spectra, taken at incident energies of 1.0 eV ($^2A_1$(C−Cl σ^*) resonance) and 4.0 eV ($^2A_1$(C−F σ^*) resonance), for instance, showed preferential excitation of the $\nu_3(a_1)$ mode (CCl_2 symmetric stretch,[30] quantum 56.7 meV[40,41]) and of the $\nu_1(a_1)$ mode (CF_2 symmetric stretch, quantum 136.5 meV[41]). The low-lying $^2A_1$ resonance also dominates DEA at low energies, yielding Cl^- anions according to the reaction

$$e^- + CCl_2F_2 \rightarrow CCl_2F_2^-{}^*(^2A_1) \rightarrow CClF_2 + Cl^- + Q \quad (3)$$

with an exothermicity of Q (298 K) = 0.15(11) eV. Accordingly, the CCl_2 symmetric stretch mode $\nu_3(a_1)$ should be active in the primary attachment process for reaction 3.

Low-energy electron attachment to CCl_2F_2 has been studied quite extensively, by both electron swarm[16,20,42−46] and electron beam methods.[8,16,31−39,47] For work carried out prior to 1997, we refer the reader to the review of Christophorou and Olthoff.[16] The swarm experiments yielded thermal attachment rate coefficients (i.e., equal electron temperature T_e and gas temperature T_G) at temperatures close to T = 300 K that scatter over the range (0.7−3.2) × 10^{-9} cm^3 s^{-1}.[16,13,46] With rising temperature, the thermal rate coefficients were found to increase with an Arrhenius-type behavior $k(T) = A \exp(-E_a/(k_B T))$ (k_B = Boltzmann constant), yielding an activation energy E_a of about 150 meV.[20,42] The data of Smith et al.[42] were extended to temperatures below 300 K by LeGarrec et al.[44] Very recently, Miller et al.[46] studied the rate over the broad temperature range 291−1100 K; they obtained an activation energy of 126(20) meV.

DEA yields for anion formation from CCl_2F_2 have been measured in electron beam experiments at resolutions of (0.05−0.5) eV.[8,16,31−39,47] At energies below about 2.0 eV (essentially only formation of Cl^-), the attachment spectra either showed a single rather broad peak or a combination of a resolution-limited peak close to 0 eV and a broader peak with a maximum in the range 0.6−1.1 eV.[16] Swarm-unfolded data indicated a further maximum around 0.3 eV.[16] Absolute cross sections around 6 × 10^{-21} m^2 have been reported[8,31,34] for energies close to 0.7 eV. The near-zero energy peak was found to depend strongly on gas temperature, indicating an activation energy of about 120 meV[35] and 100(30) meV[48] while the peak at the higher energy appears to be almost independent of gas temperature.[38,39,48] Toward higher energies, around 3.5 eV, another prominent attachment band, associated with the a_1(C−F σ^*) resonance, is observed; it yields mainly F^- and CCl_2F^- and to a lesser extent Cl_2^- and ClF^- anions.[37] Reliable absolute partial cross sections are yet to be determined.

In the present work, we combine results from high resolution laser photoelectron attachment measurements with data from two medium resolution experiments, aiming at a determination of improved partial absolute cross sections for anion formation in electron collisions with CCl_2F_2 over the range 0−12 eV at gas temperatures around 300 K. In Section II, we briefly describe the experimental setups and methods. In Section III, we provide the essentials of the R-matrix calculations. In Section IV, we report the experimental results and compare them with previous experimental work and with the results of the R-matrix calculations. In Section V, we conclude with a brief summary.

II. Experimental Methods

II.1. Laser Photoelectron Attachment Experiment (Kaiserslautern). To measure highly resolved cross sections for anion formation in low-energy electron collisions with CCl_2F_2, we used two variants of the LPA method, as discussed elsewhere in detail.[23,49−52] The energy range 1−200 meV was covered at a resolution of about 2 meV by the standard LPA method:[23,49] energy-variable photoelectrons (typical current 40 pA) are created in the reaction region with the target gas by resonant two-color photoionization of ground-state potassium atoms via the excited K(4p $^2P_{3/2}$) level.[51] Higher electron energies were accessed by the extended laser photoelectron attachment (EXLPA) method:[23,52] here near-zero energy photoelectrons are produced in an auxiliary photoionization chamber (distance from reaction center about 5 cm), accelerated by a weak electric field in a guiding magnetic field (0.002 T), brought to the energy of interest prior to traversal through the target region, and subsequently accelerated and deflected onto a collector plate.

Care was taken to align the exciting and the focused ionizing laser (diameter 0.12 mm) to avoid any collisions of the electron beam with surfaces on its way from the photoionization chamber to the collector since these would yield spurious low-energy electrons and thus lead to unwanted attachment processes. This is especially critical in energy ranges where the attachment cross section is small. In this way, the drop of the SF_6^- cross section, for example, could be followed over 5 orders of magnitude toward higher electron energies.[23,52] The effective resolution in the EXLPA experiment was about 20 meV.

Both the LPA and the EXLPA experiment were pulsed at a rate of 100 kHz; following each photoelectron production and attachment period, the infrared laser (767 nm), exciting the K(4s−4p $^2P_{3/2}$) transition, was switched off by an acousto-optical modulator, and a voltage pulse was initiated to extract the anions. A stack of electrodes imaged the anions onto the entrance hole of a quadrupole mass spectrometer (QMS) which mass selected the species of interest. The transmitted anions were detected by a channel electron multiplier (Fa. Sjuts, background 0.02/s).

A diffuse low density target of CCl_2F_2 molecules at the gas temperature $T_G = 300$ K was used. In view of the large DEA cross section for the process Cl^-/CCl_4 (the thermal rate coefficient for electron attachment to CCl_4, $k(300\ K) = 3.79(19) \times 10^{-7}$ cm^3 s^{-1} [12] at equal gas and electron temperature, exceeds that for CCl_2F_2 at 300 K by at least 2 orders of magnitude, see below), the purity of the CCl_2F_2 gas is an important issue. Using gas chromatography and Fourier-transform IR spectroscopy, we estimate that the CCl_4 fraction in the gas is below 0.1%.

The LPA/EXLPA experiment provides a highly resolved yield $Y(E)$ for anion formation. This yield is proportional to the absolute DEA cross section, that is, $\sigma(E) = NY(E)$ where N is a normalization factor, assumed to be independent of electron energy E. The size of the normalization factor is established with reference to a known thermal DEA rate coefficient for the same process. The thermal rate coefficient $k = \langle v_{rel}\, \sigma(v_{rel})\rangle$ (v_{rel} = relative collision velocity of the electron-molecule system) is given by the average[2,5,49]

$$k(T_e,T_G) = (2/m)^{1/2} \int E^{1/2}\sigma_{tot}(E;T_G)\, f(E;T_e)\, dE \qquad (4)$$

Here, T_G denotes the rovibrational temperature of the target gas, T_e is the electron temperature, and $f(E;T_e)$ is the electron distribution function. Note that the velocity of the gas molecules at $T_G = 300$ K is much smaller than the electron velocity even at electron energies as low as 0.1 meV, and the relative collision velocity v_{rel} can be replaced by the electron velocity. In calculating the rate coefficient, we use a Maxwellian distribution function which is given by

$$f(E;T_e) = 2(E/\pi)^{1/2}\beta^{-3/2} \exp(-E/\beta) \qquad (5)$$

with $\beta = k_B T_e$ (k_B = Boltzmann constant). The usual thermal average implies $T_e = T_G$ in eq 4.

For the calibration of the absolute DEA cross section scale of our LPA anion yield, we have used a thermal rate coefficient $k(T)$ at $T = T_e = T_G = 300$ K which was determined from an analysis of several temperature dependent measurements of $k(T)$,[42−46] as summarized in Figure 1. The curve represents a fit to the experimental data, assuming a modified Arrhenius-type temperature dependence

$$k(T) = k_0 + k_1 \exp(-E_A/k_B T) \qquad (6)$$

which has been suggested by recent theoretical analyses of the temperature dependence of rate coefficients for electron attachment processes.[19] The parameter k_0 is the s-wave attachment rate coefficient for the molecule of interest in the limit of very low temperature at which all molecules are in the vibrational ground state. For a molecule with a weak dipole moment (such as CCl_2F_2), the attachment cross section at very low energies is close to that for Wigner s-wave capture in a short-range force field, that is $\sigma(E) \propto E^{-1/2}$,[53] and thus the rate coefficient (eq 4) is (nearly) constant, representing the limiting ($E \rightarrow 0$) value for ground state molecules.[19] The parameter k_1 is the rate coefficient of that part of $k(T)$ which exhibits an Arrhenius-type temperature dependence with the activation energy E_A as a parameter which describes the average slope over the experimental temperature range.[19] Fits with essentially identical results and an activation energy of $E_A = 115(6)$ meV were obtained when various uncertainties for the individual data points (not always stated in the references) were used. For $T = 300$ K, the fit gives a rate coefficient $k(300\ K) = 2.2 \times 10^{-9}$ cm^{3}s^{-1} to which we assign an uncertainty of $\pm 0.8 \times 10^{-9}$ cm^{3}s^{-1}, chosen such that most of the thermal measurements are covered. Our fitted activation energy is slightly smaller than the value 126(20) meV obtained by Miller et al.[46] from a fit to data over the range 291−1100 K; this is because our fit also included data toward lower temperatures (see Figure 1).

II.2. TEM-TOF Experiment (Belfast). The DEA experiments at Belfast used a trochoidal electron monochromator (TEM) in combination with a time-of-flight (TOF) mass spectrometer. The apparatus has been described before in some detail,[54] and only the essentials are summarized here. The electron beam path is immersed in a parallel guiding magnetic field of 0.008 T. A deflection plate in the beam-monitoring Faraday cup moves the electrons off-axis and thus prevents return of the electrons to the interaction region. The electron energy was set by floating the electron gun potentials relative to the interaction region. A plate near the filament is pulsed to send short (duration about 1 μs) pulses of electrons through the interaction region. A repeller plate is pulsed to push the

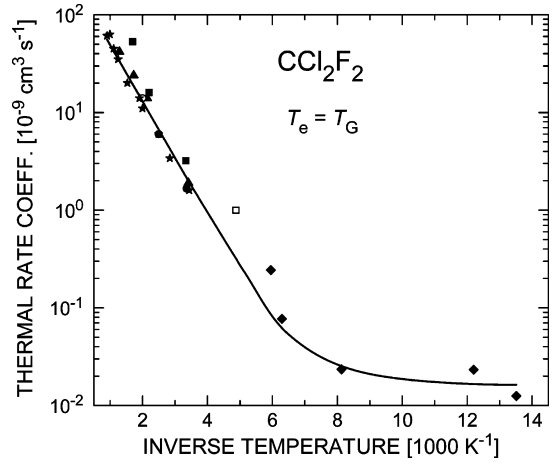

Figure 1. Arrhenius-type plot of experimental rate coefficients $k(T_e = T_G)$ for electron attachment to CCl_2F_2: full (open) squares,[20,42] full triangles,[43] full diamonds,[44] full (open) circles,[45] full asterisks[46] (open symbols represent upper limits). The full curve is the fit to the full data points, yielding the activation energy $E_A = 115(6)$ meV and the mean rate coefficient $k(300\ K) = 2.2(8) \times 10^{-9}$ cm^3 s^{-1} which was used to calibrate the absolute LPA cross section (see text).

product anions from the source region into the acceleration region of the TOF mass spectrometer after all the electrons have left the interaction region. The anions are further accelerated in the acceleration region before they pass through a field-free drift region and strike the multichannel plate (MCP) detector (anion impact energy about 0.7 keV). The repetition rate of this pulse scheme is 12 kHz. The apparatus is operated under conditions where at most one ion is detected per ten cycles to minimize any paralysis of the detector due to the arrival of two ions at the same time. All quoted anion intensities correspond to the integrals over the respective isotopic distribution. The electron energy resolution (fwhm) was estimated from the width of the apparent SF_6^- yield due to electron attachment to SF_6 at near-zero energies and in the presented measurements amounted to about 260 meV. Accordingly, the electron energy scale was calibrated by setting the energy position of the SF_6^- zero energy peak maximum to 26 meV.[55]

The experiment was carried out at room temperature (T_G = 300 K). CCl_2F_2 with a stated purity of 99.0% was provided by Argo International Ltd.. This sample was used without further purification.

II.3. TEM-QMS and TEM-TOF Experiments (Fribourg). For the DEA experiments in Fribourg two crossed electron/neutral beam apparatuses were utilized. A more detailed description of these setups can be found in refs 56−58. Both experiments were run with the gas sample previously used in Kaiserslautern.

The TEM-QMS setup[56] (subsequently addressed as "Fribourg QMS") uses a TEM to create the electron beam that then passes through a static gas target. Transmission spectra can be recorded by monitoring the current to the collector. Ions created by DEA to the gas target are drawn out through a hole in the target chamber by a three element lens and focused onto a QMS. The main coils for creating the guiding magnetic field (0.01 T) are inside the vacuum recipient and supplemented with two correction coils perpendicular to each other and to the main coils, which allow for fine-tuning of the direction of the magnetic field and thus the elimination of energy-dependent structure in the electron beam caused by interaction with the electrodes. Heating caused by the current through the coils leads to a temperature of 358 K in the reaction region. Typical operating conditions for the TEM yielded an energy width around 100 meV at an electron current of 10 nA. The base pressure of the apparatus was about 5×10^{-7} mbar; sample gas was introduced to a pressure around 1×10^{-3} mbar in the target chamber.

The energy scale for anion formation in the various attachment bands was calibrated to within 0.02 eV by simultaneously measuring $N_2^-(^2\Pi_g)$ resonance structure in the transmitted electron current (adopting 2.440(15) eV for the energy of the $N_2^-(^2\Pi_g, v = 2)$ peak[59]) and the peak locations in the yield for the various anions, using a mixed target containing suitable fractions of CCl_2F_2 and N_2. An alternative energy calibration by studying O^- formation due to DEA to CO_2 via the $^2\Pi_u$ resonance prior to measuring DEA to CCl_2F_2 gave compatible results.

The second experiment ("Fribourg TOF")[58] consists of a newly constructed TOF ion spectrometer combined with a TEM and is based on the total ion collection apparatus described previously.[57] A short (200 ns) pulse of electrons is sent through the interaction region (gas temperature 333 K) while the ion repellers are on the potential of the chamber. A 4 μs long pulse with an amplitude of −300 V is applied to the repellers about 200 ns later, after the electrons have left the collision chamber. The anions enter the TOF tube through a slit in the wall of the target chamber. The experiment is repeated at a rate of 40 kHz. The TOF tube consists of a three-cylinder electrostatic lens, which images the ion exit slit onto the MCP detector (anion impact energy 3 keV, see also ref 58). The first section of the TOF tube is split into two electrostatic deflectors, used to compensate the effect of the magnetic field. The second section of the TOF tube is used to control the focusing. The third section of the TOF tube consists of a field free flight tube.

The pressure in the collision chamber is measured by a capacitance manometer and was kept typically in the range $(3-6) \times 10^{-4}$ mbar. The energy scale was calibrated on the onset of O^-/CO_2 DEA band at 3.99 eV. The electron beam current was typically 20−80 nA and the resolution 200 meV. For the determination of absolute cross sections, the entire TOF setup was verified by measuring the DEA cross sections for O^- formation from N_2O, O_2, and CO_2; for the absolute calibration, we used the cross section 14×10^{-24} m^2 for the 4.4 eV band of O^- production from CO_2.[58]

III. R-matrix Calculations of the DEA Cross Section for Cl^- Formation from CCl_2F_2

With the aim to provide some insight into the electron attachment process we have carried out semiempirical R-matrix calculations of the DEA cross sections. Low-energy inelastic electron scattering by CCl_2F_2 is dominated by a shape resonance of a_1 symmetry, as introduced above. One should expect that this resonance drives only totally symmetric vibrations: C−F stretch, symmetric C−Cl stretch, and symmetric CCl_2 bend (or so-called scissors). However, dissociation of the temporary anion $CCl_2F_2^-$ toward $Cl^- + CClF_2$ is an asymmetric process, therefore for a rigorous calculation of the DEA process a multimode treatment, including the interaction between the vibrational modes, is necessary. In the present work, to describe the correct threshold behavior of the DEA cross section, we employ the R-matrix method,[60] and because of its complexity in the multimode case we use the one-mode approximation. First, we identify the symmetric vibrational mode that is most important for the DEA process. On the basis of the present experimental finding of a substantial channel interaction between the primary attachment process and vibrational excitation of the symmetric CCl_2 mode ν_3 (see Section IV.1), we assume that the electron capture initially drives the ν_3 mode and that the primary temporary anion state is stabilized rapidly by motion along the ν_3 coordinate. Then, mediated by intramolecular vibrational energy redistribution, the excess energy is channeled into the C−Cl stretch that eventually leads to the dissociation into the fragments Cl^- and $CClF_2$. The attachment process is thus treated in a one-dimensional approximation, assuming coupling of the anion state with only the ν_3 mode. This approach is similar to our effective-range-theory treatment of electron attachment to SF_6.[61]

We represent the neutral molecule by an effective one-dimensional potential energy curve generating the correct quantum of the ν_3 vibration, $E(\nu_3) = 56.7$ meV.[40,41] From the value of the force constant (3.724×10^5 dyn/cm[62]), we obtain the reduced effective mass $M = 28.04$ u for the ν_3 motion. For the dissociation energy, we adopt the value $D_0^{298}(CClF_2 - Cl) = 3.46(11)$ eV.[15] Using the input data described above, we parametrize the neutral curve in the Morse form

$$V(\rho) = D_e[\exp(-a\rho) - 1]^2 \qquad (7)$$

where $\rho = R - R_e$ is the normal ν_3 coordinate relative to the equilibrium separation R_e, $D_e = D_0^{298} + E(\nu_3)/2$, and $a = 0.9382$ a_0^{-1}. The anion curve is parametrized in the form

$$U(\rho) = B\exp(-2b\rho) - C\exp(-b\rho) + F \qquad (8)$$

The asymptotic value of the anion curve ($F = -0.12$ eV) was obtained from the dissociation energy D_e and the well-known electron affinity EA(Cl) = 3.6127 eV.[14] For the parameter $E_r = B - C + F$, characterizing the resonance energy at the equilibrium internuclear separation, we adopted the value 0.9 eV. After calculation of the resonance shift Δ_r due to the interaction of the resonance state with the electron continuum, we obtain for the vertical attachment energy VAE = $E_r + \Delta_r$ = 0.98 eV, which corresponds to the measured value.[10] All other parameters were considered as empirical.

The R-matrix surface amplitude $\gamma(\rho)$, which determines the resonance width,[60] was parametrized in the form

$$\gamma(\rho) = \gamma_0/[\exp(\zeta\rho) + \eta] \qquad (9)$$

where γ_0, ζ, and η are fit parameters. Typically, $\gamma(\rho)$ is a slowly varying function, and its value between the equilibrium separation ($\rho = 0$) and the crossing point between the neutral and the anion potential curves determines the absolute magnitude of the DEA cross section. The parameters employed in our calculations for the anion curve are $b = 0.7602\ a_0^{-1}$, $B = 3.092$ eV, $C = 2.071$ eV, resulting in a (classical) barrier height (energy of the crossing point between $V(\rho)$ and $U(\rho)$ above the minimum of the neutral potential) of 0.202 eV. The parameters of the surface amplitude were fixed with two objectives regarding the experimental results, (i) reproduction of the thermal rate coefficient (relevant electron energy range 0−0.2 eV) and (ii) reproduction of the shape and absolute size of the DEA cross section, reported at $T_G = 338$ K by Aflatooni and Burrow[8] (energies 0.2−1.6 eV). In this way, we obtained $\gamma_0 = 0.4960\ (a_0 \times \text{hartree})^{1/2}$ (1 hartree = 27.211 eV), $\zeta = 1.051\ a_0^{-1}$, and $\eta = 2.678$.

The vibrational motion for the calculation of the DEA cross sections was included, using the quasiclassical approximation of the R-matrix theory.[60,63] To couple the resonant anion state with the electron continuum, we calculate the electron wave functions in electron scattering channels. For these calculations on CCl_2F_2, we have employed the dipole moment $\mu = 0.51$ D[15] and the polarizability $\alpha = 53.5\ a_0^3$.[15]

IV. Results and Discussion

IV.1. Highly Resolved Absolute Cross Section for Cl^- Formation in DEA to CCl_2F_2 Molecules ($T_G = 300$ K). In agreement with the earlier work,[32−39] the present experiments in Belfast, Fribourg, and Kaiserslautern confirm that Cl^- is by far the dominant anion formed in electron attachment to CCl_2F_2 at low energies ($E < 2$ eV). In the following we discuss the highly resolved LPA and EXLPA results that were obtained for the Cl^- anion over the range 0.001−1.8 eV. As explained in Section II.1, the absolute scale of the cross section for Cl^- formation was determined with reference to the rate coefficient $k(300\text{ K}) = 2.2(8) \times 10^{-9}$ cm^3 s^{-1}.

In Figure 2, we present the absolute DEA cross section for Cl^- formation due to electron attachment to CCl_2F_2 molecules (gas temperature $T_G = 300$ K). It was obtained by combining the LPA (1.2−164 meV) and the EXLPA (20−1800 meV) data, normalizing the EXLPA results to the LPA data in the energy range from 40 to 150 meV. The energy resolution was about 2 meV for the LPA data and about 20 meV for the EXLPA results. Below 0.5 eV the partial Cl^- cross section is identical with the total cross section; therefore, it is possible to use the total thermal

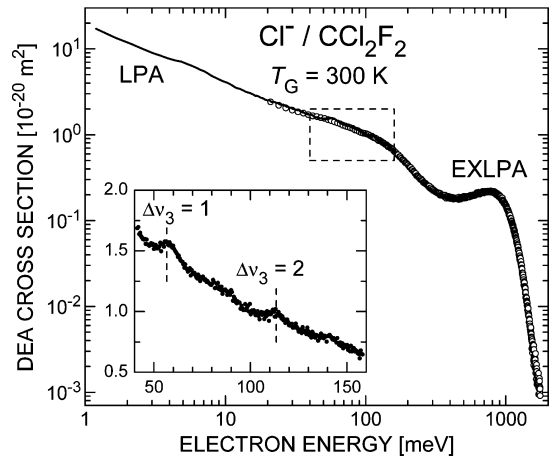

Figure 2. Absolute cross section for Cl^- formation due to electron attachment to CCl_2F_2 (gas temperature $T_G = 300$ K), full curve, LPA data (1.2−164 meV); open circles, EXLPA data (20−1800 meV). The insert presents a magnified view of the LPA data (full circles), exhibiting cusp structure which occurs at the thresholds for vibrational excitation (VE) of one and two quanta of the $\nu_3(a_1)$ mode (≈56.7 and ≈113 meV, respectively) and which is due to interaction between the attachment and the VE channel.

rate coefficient $k(T = 300\text{ K})$ to establish the absolute cross section scale shown in Figure 2.

Cusp structure due to the interaction of the attachment channel with the VE process is observed, most notably peak-like features around $E = 57$ meV and $E = 114$ meV (see insert in Figure 2); the vertical dashed lines indicate the thresholds for excitation of one ($\nu_3 = 1$; 56.7 meV)[40,41] and two quanta ($\nu_3 = 2$) of the vibrational modes in CCl_2F_2. As is known from the previous high resolution work on molecules such as SF_6,[49] CCl_4,[22] and $CHCl_3$,[64] these Wigner cusps are characteristic for the vibrational modes which are active in the attachment process. Note that for Cl^- formation, the vibrational modes which may be considered to promote dissociation of the primary anion complex $[CCl_2F_2]^-$ toward the fragments $Cl^- + CClF_2$ are not identical with the channel interaction mode $\nu_3(a_1)$, which represents the symmetric stretch C−Cl_2 mode with a_1 symmetry which is compatible with s-wave electron attachment.

From 0.1 to 0.3 eV, the cross section drops by about a factor of 5, while it varies rather little from 0.3 to 0.9 eV with a shallow minimum around 0.4 eV and a maximum around 0.78 eV. From 0.9 to 1.8 eV, the cross section decreases monotonically by a factor of about 200. Over the range 0.5−1.8 eV, the shape of the EXLPA cross section is in good agreement with that reported for the total cross section by Aflatooni and Burrow at $T_G = 338$ K,[8] but the absolute values of the latter are about a factor of 2.5 higher. This difference cannot be explained by other anion channels; at energies above 0.5 eV Cl_2^- ions are formed in addition, but only at a fraction of about 1%. Other measurements of the total cross section around 0.7 eV also provided values much higher than the EXLPA result (see the comparative discussion of the total cross sections in Figure 6 below). The DEA cross section of Aflatooni and Burrow[8] at energies around 0.7 eV is further supported by a new accurate measurement of the absolute value with the Fribourg TOF apparatus (see Table 1 and Section IV.4).

Toward smaller energies, the EXLPA and the total cross section[8] come into closer agreement and nearly merge around 0.15 eV. All these findings suggest that the EXLPA cross section becomes progressively too low toward larger energies and that this change mainly occurs over the range 0.15−0.5 eV. A

TABLE 1: Absolute Cross Sections and Branching Ratios for Anion Formation Due to Electron Attachment to the Molecule CCl_2F_2 (Rovibrational Temperature $T_G \approx 300$ K)

anion	peak position [eV]	peak maximum [10^{-21} m^2]	peak width (fwhm) [eV]	branching ratio (max)
Cl^-	Zero Energy Peak			
LPA[a]	0.001	191		
ΔE_{80}[b]	0.017	24.9	0.12	
ΔE_{260}[b]	0.050	11.5	0.32	
Cl^-	2nd Peak			
EXLPA	0.78	2.2[c]		
Lincoln[d]	0.71	5.44		
Belfast[e]	0.76	[5.44]		11.52
Fribourg TOF[f]	0.75	5.54 ± 7%		11.84
Berlin[g]	0.58			20.24
Berlin[h]	0.55(10)		≈0.55	7.25
Cl^-	3rd Peak			
Belfast[e]	3.25; 4.18	0.044; 0.027	1.85[i]	0.093; 0.056
Fribourg TOF[f]	3.25; 4.18	0.055; 0.030		0.118; 0.065
Fribourg QMS[f]	3.25; 4.06	±7%	1.85[i]	0.105; 0.106
Berlin[h]	≈3.0; ≈3.8		≈1.8 [i]	
F^-				
Belfast[e]	3.25	0.477	0.98	1
Fribourg TOF[f]	3.25	0.468 ± 8%	1.10	1
Fribourg QMS[f]	3.25		0.98	1
Berlin[g]	3.1		0.94	1
Berlin[h]	3.1(2)		≈1.1	1
CCl_2F^-				
Belfast[e]	3.68	0.125	0.85	0.262
Fribourg TOF[f]	3.65	0.205 ± 8%	1.00	0.438
Fribourg QMS[f]	3.66		0.82	0.235
Berlin[g]	3.5		0.98	0.193
Berlin[h]	3.55(2)		≈1.0	0.31
Cl_2^-				
Belfast[e]	0.91; 3.25	0.022; 0.008	0.55; 1.1	0.046; 0.017
Fribourg TOF[f]	0.90; 3.20	0.0175; 0.0096	0.66; 1.17	0.037; 0.021
Fribourg QMS[f]	0.92; 3.31	±9.5%	0.56; 1.1	0.118; 0.016
Berlin[g]	0.78; 3.12		0.54; 0.92	0.136; 0.025
Berlin[h]	0.65(10); ≈3.1		≈0.6; ≈1.2	≈0.12; ≈0.03
FCl^-				
Belfast[e]	3.59	0.006	1.0	0.013
Fribourg TOF[f]	3.6	0.0064 ± 7.5%	0.92	0.014
Fribourg QMS[f]	3.60		1.0	0.034
Berlin[g]	3.38		0.88	0.029
Berlin[h]	2.85(20)		≈0.9	0.16

[a] LPA peak position and maximum are given for $E = 1$ meV (the cross section is divergent for $E \to 0$). [b] LPA cross section convoluted with Gaussian energy resolution functions of fwhm = 80 and 260 meV, respectively. [c] EXLPA cross section too low due to discrimination effects (see text). [d] Measured total cross section;[8] other fragments negligible in this energy range (see text). [e] Cross sections of the Belfast TEM-TOF experiment normalized to the 2nd Peak of ref 8. [f] Fribourg TOF: TEM-TOF experiment ($T_G = 333$ K). Fribourg QMS: TEM-QMS experiment ($T_G = 358$ K). [g] Reference 37. [h] Reference 32. Branching ratios for energy integrated intensities; values given with "≈" estimated from Figures 3−5 in this reference. [i] Double peak structure of 3rd peak not resolved; width given for total structure.

possible explanation for this discrepancy is the presence of a substantial, energy-dependent discrimination effect in the EXLPA experiment for Cl^- formation from CCl_2F_2. Such an effect could be explained by a strong rise in the kinetic energy of the Cl^- ion with increasing electron energy which would occur if a large fraction of the energy sum $E + Q$ (exothermicity $Q = 0.15$ eV, see above) appears as kinetic energy of the DEA fragments. Kinematically, the maximum kinetic energy of the Cl^- ion is given by $(M_{CClF2}/M_{CCl2F2})(E + Q) \approx 0.71\ (E + Q)$ if we ignore the initial translational and rovibrational energy of the molecule (M_{CClF2} and M_{CCl2F2} are the masses of the fragment $CClF_2$ and of CCl_2F_2, respectively). When the electron energy rises from 0 to 0.8 eV, the maximum kinetic energy of the Cl^- ion increases from about 0.11 to 0.68 eV, and this increase may result in a substantial decrease of the anion detection efficiency. If part of the available excess energy is transformed into internal energy of the $CClF_2$ fragment, the effect will be reduced, but may still be significant. We note that, using TOF analysis of the anions, Illenberger[33] in fact demonstrated variations in the kinetic energies of the Cl^- ions with electron energy, but the data are not sufficiently detailed to allow simulations of the discrimination effects for the present EXLPA experiment.

In this connection, we note that in the recent work on DEA to $CHCl_3$[64] a similar deviation between the EXLPA cross section for Cl^- formation and the total cross section reported by Aflatooni and Burrow[7] was observed. The case is different from CCl_2F_2, however, since the second maximum (i.e., that above the zero energy peak) occurs at a lower energy (0.37 eV) and the exothermicity for Cl^- formation at $E = 0$ eV is higher (0.39 eV) for $CHCl_3$. Correspondingly, one expects the discrimination effects in the EXLPA data for $CHCl_3$ to be smaller than for CCl_2F_2. Yet, at least part of the observed deviation (the EXLPA peak cross section being 42% lower)[64] may be due to discrimination effects in the EXLPA experiment.

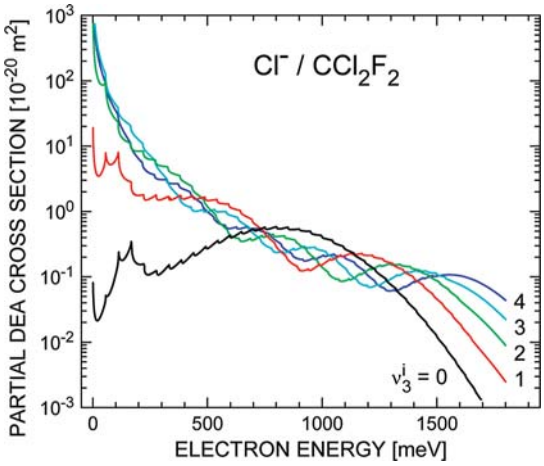

Figure 3. Calculated state-specific partial absolute DEA cross sections for CCl_2F_2 molecules in the initial vibrational level $\nu_3^i = 0-4$.

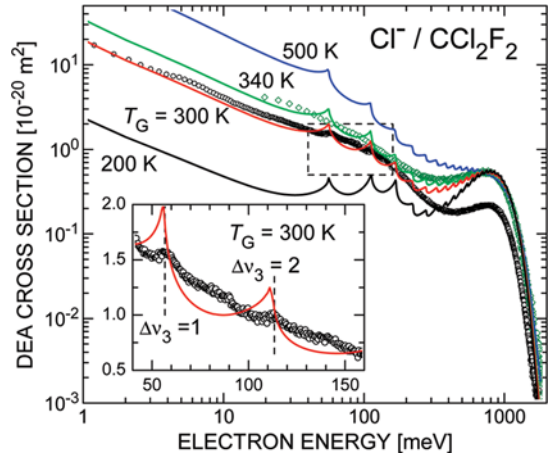

Figure 4. Calculated, thermally averaged DEA cross sections for Cl^- formation, obtained with initial vibrational state populations for temperatures of $T_G = 200$, 300, 340, and 500 K, in comparison with the experimental data measured at $T_G = 340$ K (open diamonds)[8] and $T_G = 300$ K (open circles, LPA/EXLPA, this work). The insert presents a magnified view of the LPA data (full circles) in comparison with the calculated cross section (full curve, $T_G = 300$ K), both exhibiting cusp structure that occurs at the thresholds for vibrational excitation (VE) of one and two quanta of the $\nu_3(a_1)$ mode (≈56.7 and ≈113 meV, respectively) and which is due to interaction between the attachment and the VE channel.

IV.2. Results of R-Matrix Calculations for Cl^- Formation. As stated in Section III, the R-matrix parameters were chosen such that calculations yielded (i) a thermal rate coefficient close to the fitted experimental value $k(300\ \text{K}) = 2.2 \times 10^{-9}\ \text{cm}^3\ \text{s}^{-1}$ and (ii) an absolute cross section close to that of Aflatooni and Burrow at energies around 0.7 eV ($0.54 \times 10^{-20}\ \text{m}^2$).[8] We note that the combined use of condition (i) and, instead of the requirement (ii), of a lower absolute cross section around 0.7 eV to match the EXLPA data over the full range resulted in a cross section shape at higher energies which breaks off too rapidly; this behavior signals too low a survival factor for attachment processes, occurring in the center of the Franck−Condon region.

Vibrationally averaged DEA cross sections for gas (i.e., vibrational) temperatures of $T_G = 200-500$ K (see Figure 4) demonstrate that the cross sections at the broad peak around 0.7 eV is essentially independent of the vibrational temperature. Therefore, the cross sections of the EXLPA and of the electron beam experiments[8,31,34] (see Figure 6), although taken at somewhat different temperatures, should agree at energies around 0.7 eV. As a consequence, the low cross section of the EXLPA experiment must in fact be due to the discrimination effects discussed in Section IV.1.

In Figure 3, we show DEA cross sections for Cl^- formation, computed for CCl_2F_2 molecules in the initial vibrational levels $\nu_3 = 0-4$ over the electron energy range 0.001−1.6 eV. With the R-matrix parameters used in these calculations, we obtained a thermal rate coefficient of $k(300\ \text{K}) = 2.0 \times 10^{-9}\ \text{cm}^3\ \text{s}^{-1}$ and a vibrationally averaged cross section of $5.4 \times 10^{-21}\ \text{m}^2$ at energies around 0.7 eV. The calculated DEA cross sections depend strongly on the quantum number ν_3 at low electron energies, rising from $0.25 \times 10^{-21}\ \text{m}^2$ for $\nu_3 = 0$ to $67.9 \times 10^{-21}\ \text{m}^2$ for $\nu_3 = 3$ at $E = 10$ meV. At energies around 0.8 eV, in contrast, the cross sections for $\nu_3 = 0-4$ are of similar size (around $5 \times 10^{-21}\ \text{m}^2$ to within about a factor of 2). The shape of the individual cross sections in the Franck−Condon region nicely reflects the nodal structure of the nuclear wave functions. For $\nu_3 = 1$, for instance, one observes a clear minimum in the cross section at $E \approx 0.9$ eV. For higher vibrational levels, the strong drop of the cross sections is progressively shifted to larger electron energies.

At the thresholds for vibrational excitation Wigner cusp structure is observed due to the interaction of the attachment with the VE process. These features are especially clear at the $\nu_3 = 3$ threshold in the cross sections for the initial $\nu_3 = 0$ and 1 levels for which they occur at electron energies of 168 and 113 meV, respectively. The $\nu_3 = 3$ level is located just below the crossing point between the neutral and anion curves and has the largest DEA cross section at low energies.

In Figure 4, we show thermally averaged DEA cross sections for Cl^- formation, obtained with initial vibrational state distributions for temperatures of $T_G = 200$, 300, 340, and 500 K.

At low electron energies, the vibrationally averaged cross section at $T_G = 200$ K is mainly due to the contributions from the $\nu_3 = 1$ and 2 levels (population fractions only 3.6% and 0.13%, respectively); at $T_G = 300$ K, the $\nu_3 = 2$ level (population 1.1%) provides the highest contribution while at $T_G = 500$ K, the $\nu_3 = 2$ and 3 levels (populations 3.0% and 0.58%) dominate with similar contributions. At energies around 0.7 eV, in contrast, the $\nu_3 = 0$ level (population between 96.3 and 74.5% for temperatures between 200 and 500 K) dominates the DEA cross section at all temperatures.

The thermally averaged R-matrix cross sections at the two respective gas temperatures are in good agreement with the total cross section of Aflatooni and Burrow (open diamonds, $T_G = 338$ K)[8] from 0.03 to 1.5 eV and with the EXLPA cross section ($T_G = 300$ K) from 0.001 to 0.25 eV. The Wigner cusp structure is weaker in the LPA data and washed out in the lower resolution results.[8] The more pronounced cusp structure in the theoretical cross sections is in part due to the one-dimensional character of the model used in the calculations. It is known, for example, that boomerang oscillations obtained in one-dimensional calculations for CO_2, are reduced significantly after inclusion of additional degrees of freedom.[65]

IV.3. Partial DEA Cross Sections and Branching Ratios. Figure 5 summarizes and compares the yields of the main bands for the five anions formed with notable intensities, namely (a) Cl^-, (b) F^-, (c) CCl_2F^-, (d) Cl_2^-, and (e) FCl^-, as measured in Belfast (open circles; energy width 260 meV, gas temperature $T_G = 300$ K) and with the Fribourg QMS setup (full curves; energy width about 100 meV, gas temperature $T_G = 358$ K) and normalized to one of the respective band maxima, as indicated in Figure 5. The Fribourg QMS data possess a high

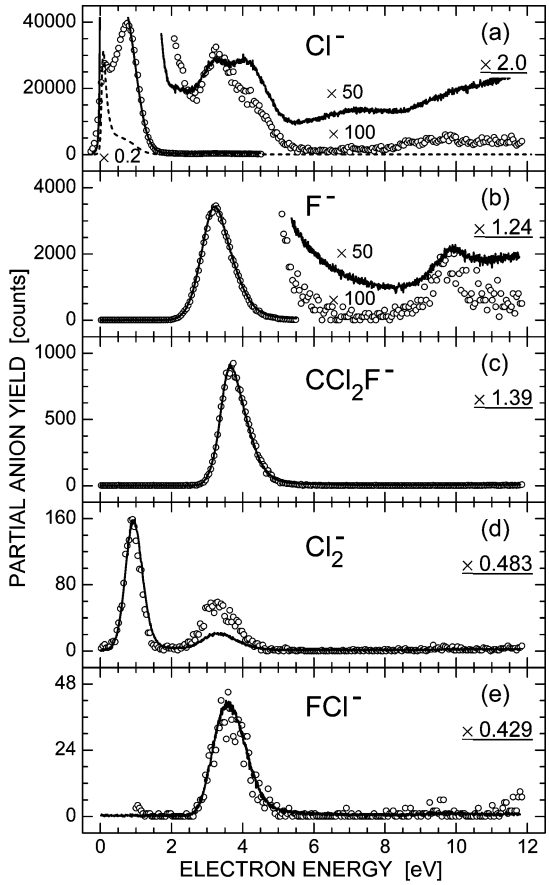

Figure 5. Partial anion yields for DEA to CCl_2F_2 ($E = 0-12$ eV), yielding the fragment anions (a) Cl^-, (b) F^-, (c) CCl_2F^-, (d) Cl_2^-, and (e) FCl^-, as measured in Belfast (open circles) at $T_G = 300$ K and in Fribourg (full curves) at $T_G = 358$ K. The Fribourg QMS data have been normalized to one of the Belfast band maxima, the respective normalization factors are shown underlined on the right side of the graphs. In (a) and (b) both data sets have been magnified at larger electron energies by the factors indicated in the middle of the graphs; for Cl^- (a), the Fribourg QMS data have been demagnified at the lowest electron energies (broken curve) by a factor of 5 (i.e., a total factor of 10 with respect to the Belfast data) to show its huge zero energy peak (see text).

signal-to-noise ratio and thus characterize the band shapes in detail. Except for the near-zero energy band for Cl^- (see below), the band shapes and the energy locations of the respective band maxima are found to be in good agreement between the two data sets, whereas the Belfast branching ratios differ by factors between 0.38 and 1.1 from the Fribourg QMS data (see Figure 5 and Table 1). The differences in the near-zero energy behavior are due to the experimental resolution and to the gas temperatures. With rising temperature, the near-zero energy peak rises strongly[16,35−39] (see also the results of the R-matrix calculations); with broader energy width the near-zero energy peak is suppressed. Thus, both effects promote the occurrence of a strong near-zero energy peak in the Fribourg QMS data. Spectra taken at Belfast with improved resolution also showed a near-zero energy peak, although of lower strength than expected when compared with the convoluted LPA data (using $\Delta E_{fwhm} = 260$ meV, see Table 1, "zero energy peak"). We emphasize that the strength of the near-zero energy peak in an attachment yield, measured in most electron beam experiments (except for the LPA experiment), is questionable for several reasons, as discussed in some detail in refs 64 and 66.

Satisfactory overall agreement is also found in the shapes and energy locations of the bands for the five anions observed at Berlin by Langer et al.[37] (energy width about 250 meV). Closer inspection indicates a general shift of the bands measured at Berlin to lower electron energies by about 0.15 eV (see Table 1); this shift may stem from a cutoff at very low energies, such that the near-zero energy feature in the Cl^- yield actually corresponded to a corrected energy of about 0.15 eV. We note that the energy dependence for the first band in the Cl_2^- yield, as measured with the (EX)LPA method, is in close agreement with that observed in Belfast and Fribourg. If the three data sets of Berlin, Belfast, and Fribourg QMS are compared on a logarithmic yield scale, it is found that the Belfast data exhibit lower background signal than those of Fribourg QMS and especially those of Berlin. In the latter data, the third peak for Cl^- formation is obscured by background signal.

In Table 1, we summarize several properties of the various attachment bands, namely peak energy positions, absolute maximum cross sections (only for the Belfast and Fribourg TOF experiments), peak widths, and band branching ratios, as observed in the present and two earlier[32,37] experiments. The branching ratios are normalized to 1 for the isolated F^- band which peaks at 3.25 eV. This choice was made to circumvent the problems associated with the different shapes of the Cl^- band around 0.7 eV.

An excellent overall agreement (typically ±20% or better) between the branching ratios of the two TEM-TOF experiments in Belfast and Fribourg is observed (except for the CCl_2F^- fragment for which the Fribourg TOF cross section is 67% higher). On the one hand, this agreement is expected from the similar design of the two TEM-TOF experiments which sample all the anions and, therefore, discrimination effects associated with differences in the kinetic energy spectra and angular distributions of the various fragment anions are minimized. On the other hand, this agreement documents that the (relative) detection efficiencies of the various anions in these two TOF experiments are essentially identical although the anion impact energies at the MCP detector of the Fribourg TOF experiment (3 keV) are much higher than those at the Belfast MCP detector (0.7 keV). The 67% difference observed for the heaviest detected fragment anion CCl_2F^- may be due to a reduced MCP detection efficiency in the Belfast experiment.

The agreement between the Belfast and Fribourg TOF data also demonstrates that the influence of the two slightly different gas temperatures (300 and 333 K, respectively) on the relative intensities of these DEA bands is only weak. As recommended branching ratios we propose to use the arithmetic means from the Belfast and Fribourg TOF experiments.

The branching ratios observed in the other experiments (Fribourg QMS and refs 32 and 37; see Table 1) are found to differ more or less strongly from the Belfast and Fribourg TOF data in a way which depends on the anion and the specific band. Such deviations are not unexpected since complete anion sampling is difficult with a QMS analyzer, especially when a weak anion extraction field is used. Thus, we attribute the deviations to the discrimination effects mentioned above.

IV.4. Total DEA Cross Section for CCl_2F_2. In Figure 6, we show results for total DEA cross sections over the energy range 0−6 eV from four experiments. The full (dashed) curve reproduces the LPA/EXLPA cross section for Cl^- formation ($T_G = 300$ K) at energies $E \leq 0.2$ eV ($E = 0.2-1.8$ eV). The full diamonds represent the total cross section due to Aflatooni and Burrow[8] ($E \geq 0.05$ eV, energy width about 0.08 eV, $T_G = 338$ K). The open circles show the total cross section of the Belfast experiment ($E \geq 0.12$ eV, energy width 260 meV, $T_G = 300$ K; sum over all anion channels), as normalized to the

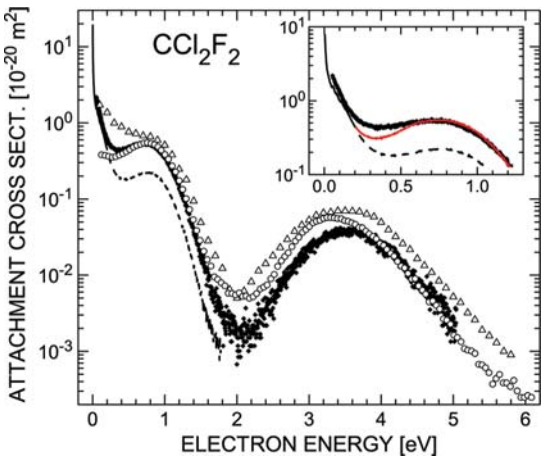

Figure 6. Total absolute experimental cross sections for anion formation in electron-CCl_2F_2 collisions over the energy range 0−6 eV (gas temperatures near T_G = 300 K); open triangles,[31] (≈400 K); full diamonds,[8] (338 K); open circles, Belfast (300 K); full curve, LPA/EXLPA (300 K, $E \leq 0.2$ eV); broken curve, LPA/EXLPA (300 K, $E > 0.2$ eV). The inset presents a magnified view of the minimum between the zero energy peak and the 2nd peak around 0.7 eV; the red curve is a simple interpolation between the LPA/EXLPA data below 0.2 eV (full curve) and the data of ref 8 above 0.6 eV (full diamonds) (for details see text).

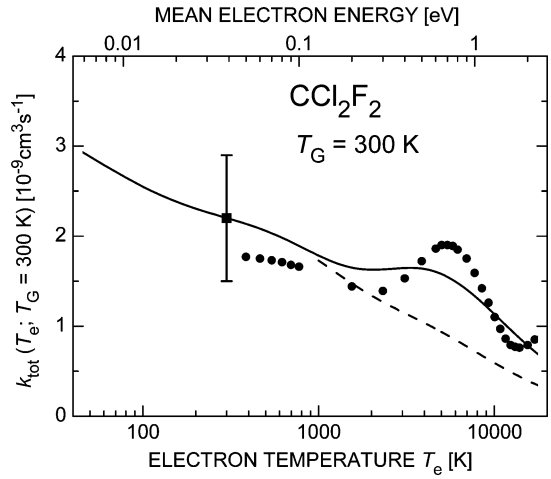

Figure 7. Dependence of the total rate coefficient for DEA to CCl_2F_2 on electron temperature T_e over the range 40−20000 K (mean electron energy $<E>$ = 0.0052−2.59 eV) at the fixed gas temperature T_G = 300 K. Full curve, rate coefficient calculated from the total DEA cross section (see text and insert in Figure 6 (red curve)); broken curve, rate coefficient calculated from the LPA/EXLPA total DEA cross section (see text and insert in Figure 6 (broken curve)); full circles, electron swarm results from ref 16. The full square denotes the thermal rate coefficient (2.2(8) × 10^{-9} cm^3 s^{-1} at $T_e = T_G$ = 300 K) which was used for calibration of the DEA cross section (see text).

total cross section of Aflatooni and Burrow[8] at the maximum near 0.71 eV. The open triangles give the total cross section measured by Pejcev et al.[31] ($E \geq 0.1$ eV, energy width about 0.2 eV, gas temperature not listed, but likely 400 K or above). All data are consistent in the strong drop of the cross section above 0.8 eV toward the more or less deep minimum, located at about 2 eV, but otherwise substantial differences are observed, in part associated with the nonidentical gas temperatures. The minimum near 0.45 eV in the T_G = 300 K EXLPA data is shifted down to about 0.3 eV in the total cross section of Aflatooni and Burrow,[8] and it is lost in the data of ref 31 (as well as in the Fribourg data, not shown here, see Figure 5a) which exhibit a broad shoulder with a minimal slope around 0.7 eV, but neither a local minimum or maximum in the range 0−0.8 eV.

The absolute values of the total DEA cross sections from three beam experiments agree within their mutual uncertainties at an energy of 0.71 eV, namely 6.8 × 10^{-21},[31] 6 × 10^{-21},[34] (T_G = 393 K, not shown in Figure 6), and 5.44 × 10^{-21} m^2.[8] The respective new value obtained at Fribourg (sum of the partial cross sections for Cl^- and Cl_2^- formation) amounts to 5.55 × 10^{-21} m^2 (±7%), in excellent agreement with that of Burrow and Aflatooni. In contrast, the local maximum around 0.75 eV in the EXLPA cross section reaches only a value of 2.2 × 10^{-21} m^2, as already discussed in Section IV.2 and attributed to discrimination effects in the EXLPA data at higher energies.

On the basis of all the experimental and theoretical evidence, a proper DEA cross section for T_G = 300 K over the range 0.001−2.0 eV contains the following elements: (i) the LPA/EXLPA cross section at energies up to 0.2 eV; (ii) the cross section of Aflatooni and Burrow for energies above 0.6 eV (where the dependence on gas temperature is negligible); (iii) an interpolated cross section joining elements (i) and(ii) over the range 0.2−0.6 eV. The insert in Figure 6 illustrates this (simple) interpolation (red curve); it involves multiplication of the original EXLPA cross section by a factor which rises linearly with electron energy from unity at 0.2 eV to 2.5 at 0.6 eV. In this range, it agrees with the calculated cross section to within 10%. This newly constructed DEA cross section will be used in Section IV.5 in the calculations of the dependence of the rate coefficient at fixed gas temperature (T_G = 300 K) on electron temperature.

IV.5. Dependence of Total Attachment Rate Coefficient on Electron Temperature. In the following, we discuss the dependence of the total DEA rate coefficient $k(T_e; T_G)$ on electron temperature T_e (40−20 000 K) for the fixed gas temperature T_G = 300 K. We calculated $k(T_e; T_G)$ with eq 4, using the newly constructed total DEA cross section for T_G = 300 K (see Section IV.4 and insert in Figure 6) and a Maxwellian electron distribution function. The computed rate coefficients $k(T_e; T_G = 300\ K)$ (full curve in Figure 7) show a decrease for electron temperatures up to about T_e = 1500 K, followed by an almost constant value up to about 4000 K and another decay toward larger temperatures. When the original EXLPA cross section is used in the calculations (broken curve), the rate coefficients are identical up to T_e = 800 K, but decrease monotonically and substantially faster toward larger temperatures.

The swarm data (T_G = 298 K, as listed in Table 16 of the review by Christophorou et al.[16]) are characterized by a clear peak (located at an electron temperature of 5500 K, i.e., mean electron energy of 0.7 eV). This peak is seen to exceed the adjacent minima (at about 2000 and 14 000 K) by about a factor of 2, a behavior which is not compatible with any of the total cross section shapes in Figure 6, even if electron distribution functions different from our assumed Maxwellian form are assumed. We note that the swarm data were measured with N_2 carrier gas at the lower electron temperatures and with Ar carrier gas for the higher temperatures.[16,45] Wang et al.[45] also measured the function $k(T_e; T_G)$ for the higher gas temperatures T_G = 400 and 500 K. As expected from the fact that the attachment cross section near zero energy increases strongly with rising gas temperature,[16,35,38,39,48] they found an increase of the rate coefficients with rising gas temperature, especially at the lower electron temperatures (see Figure 4 in ref 45).

IV.6. R-Matrix Cross Sections for Vibrational Excitation. Vibrational excitation of the CCl_2F_2 molecule by low-energy electron impact was experimentally studied in detail by Mann

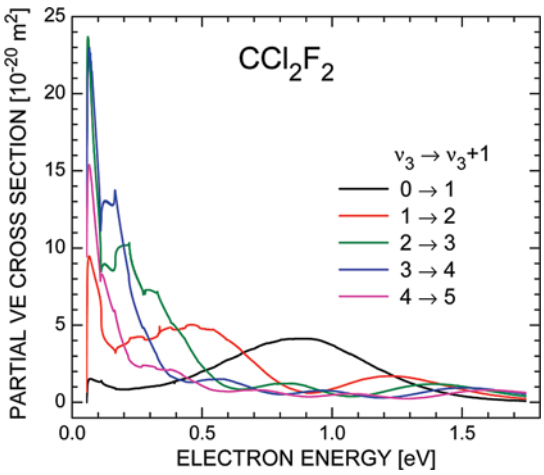

Figure 8. Calculated partial VE cross sections ($\Delta\nu_3 = 1$) for CCl_2F_2 in the initial vibrational states $\nu_3 = 0-4$.

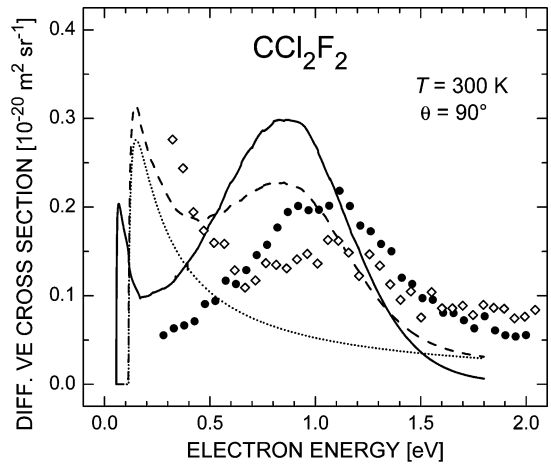

Figure 9. Calculated, thermally averaged differential cross sections for VE of CCl_2F_2 (full curve, $\Delta\nu_3 = 1$; dotted curve, $\Delta\nu_8 = 1$ (Born-dipole approximation); dashed curve, sum of $\Delta\nu_3 = 2$ and $\Delta\nu_8 = 1$ (see text)), in comparison with experimental data measured at $\theta = 90°$[30] (full circles, $\Delta\nu_3 = 1$; open diamonds, sum of $\Delta\nu_3 = 2$ and $\Delta\nu_8 = 1$).

and Linder[30] with a gas target at room temperature ($T_G \approx 300$ K[67]). They observed that in the $^2A_1$ (C−Cl) resonance region (near 1 eV) the most pronounced excitation is that of the ν_3 mode (transitions with $\Delta\nu_3 = +1$). At $T_G = 300$ K, the largest contribution stems from excitation of the ground state ($\nu_3 = 0 \rightarrow 1$), but VE of initially excited levels (mainly $\nu_3 = 1 \rightarrow 2$) cannot be neglected, and thus the proper thermal average has to be calculated for comparison with experiment. The first overtone of ν_3 ($\Delta\nu_3 = +2$ processes, labeled $2\nu_3$, energy loss $\approx$ 113 meV) is also significantly excited, but since $2\nu_3$ has almost the same energy as the CCl_2 asymmetric stretch mode ν_8 (114.4 meV) the experiment (resolution about 25 meV[30]) measures the sum of $2\nu_3$ and ν_8.

With the same set of R-matrix parameters used to compute the DEA spectra, we also calculated cross sections for VE of ν_3 and $2\nu_3$. In Figure 8 we present partial cross sections for $\Delta\nu_3 = +1$ transitions for the initial levels $\nu_3 = 0-4$. A strong dependence on the initial state is observed, especially in the near-threshold region. At higher energies (around 0.9 eV) the cross sections reflect the nodal structure of the initial vibrational wave function, see, for instance, the minimum in the $\nu_3 = 1 \rightarrow 2$ cross section. Using the partial cross sections of Figure 8, the temperature average for $T_G = 300$ K was obtained. This cross section was divided by 4π (assuming angular isotropy) to yield the differential cross section shown by the full line in Figure 9. This procedure is reasonable since the dipole moment of CCl_2F_2 is rather weak, and the $^2A_1$ resonance is dominated by the s-wave. The theoretical results are compared with the experimental differential VE cross section (90°; full circles).[30] The experimental maximum occurs at about 1 eV (uncertainty of energy scale about 50 meV[67]), about 0.15 eV higher than the location of the calculated maximum, but the cross section shapes are in good agreement. Satisfactory agreement is observed in the absolute size of the peak cross sections, particularly in view of the assumption of an isotropic angular distribution. It could be suggested that the energy position of the peak can be raised by increasing VAE. However, our corresponding attempts did not shift the peak position for VE substantially while they strongly reduced the DEA cross section. Another point of disagreement is a faster drop of the theoretical cross section with energy. This is obviously due to the single-resonance feature of our model which does not include the higher energy $^2B_2$ resonance which produces another peak in the experimental cross section at about 2.5 eV.[30]

In Figure 9, we also present the angle-differential (90°) sum cross section for $2\nu_3 + \nu_8$ excitation. The experimental data are given by the open diamonds while the dashed line represents the calculated sum. Since the ν_8 mode (b_2 symmetry) is infrared active, its excitation can be calculated using the Born-dipole model (at 90°; dotted curve). The computed total cross section for $2\nu_3$ was divided by 4π to obtain the estimate for the differential cross section (dashed curve). Again, satisfactory agreement between the experimental data and the calculated sum cross section is observed. Note that even better agreement is obtained for the ratio of the ν_3 to $2\nu_3 + \nu_8$ peak cross sections. The experiment does not reach the energy region close to threshold, and it would be of interest to have highly resolved experimental data which could test the predicted threshold behavior and Wigner cusp structure at the first and higher vibrational onsets.

V. Conclusions

A joint experimental and theoretical study of electron attachment to dichlorodifluoromethane (CCl_2F_2) molecules in the gas phase at gas temperatures near 300 K has resulted in a new, reliable set of total and partial DEA cross sections (formation of Cl^-, Cl_2^-, F^-, ClF^-, and CCl_2F^-) over the range 0−12 eV. They combine highly resolved laser photoelectron attachment data at low energies with electron beam data at higher energies. Cusp structure indicates that the CCl_2 stretch mode ν_3 is important for the initial electron capture process. Using this information and known properties of CCl_2F_2, R-matrix calculations of the DEA cross sections for molecules in different initial vibrational states ($\nu_3 = 0-4$) were carried out. The results predict the dependence of the DEA cross section on the initial vibrational level ν_3 and on the vibrational temperature; good agreement with the experimental cross sections is obtained.

Using the same R-matrix parameters, the cross section for vibrational excitation of the ν_3 mode and its harmonic $2\nu_3$ were computed. Moreover, excitation of the infrared-active ν_8 mode (very close to the energy of $2\nu_3$) was calculated in the Born-dipole approximation. The computed cross sections for ν_3 and $2\nu_3 + \nu_8$ excitation are in satisfactory agreement with experimental results.[30]

Acknowledgment. The authors acknowledge the stimulation provided for this joint project through the ESF network Electron-Induced Processing At the Molecular level (EIPAM). T.A.F.,

K.G., and S.A.H. would like to thank the EPSRC for their support of this work through Grant EP/F031025/1. The work in Kaiserslautern was supported by the Deutsche Forschungsgemeinschaft (HO 427/29) and by the Forschungszentrum OTLAP. The work in Fribourg was supported by the Swiss National Science Foundation Project No. 200020-113599/1, COST Action CM0601 and a matching fund C07.0018 of the Swiss State Secretariat for Education and Research. IIF was supported by the U.S. National Science Foundation (Grant PHY-0652866). T.H.H. gratefully acknowledges B. Ibanescu and D. Kubala for their support with the TEM-QMS experiment at Fribourg. We thank P. D. Burrow, J. Langer, and A. Mann for providing data in numerical form, T. M. Miller for providing a preprint of ref 46, and G. Seyfang for information on the vibrational spectrum of CCl_2F_2.

References and Notes

(1) *Electron-Molecule Interactions and Their Applications*; Christophorou, L. G., Ed.; Academic Press: New York, 1984; Vols. 1 and 2.
(2) Chutjian, A.; Garscadden, A.; Wadehra, J. M. *Phys. Rep.* **1996**, *264*, 393.
(3) Christophorou, L. G. Olthoff, J. K. *Fundamental Electron Interactions With Plasma Processing Gases*; Kluwer Academic/Plenum Publ.: New York, 2004.
(4) Illenberger, E. In *Photoionization and Photodetachment Part II* (Adv. Ser. Phys. Chem.); Ng, C.-Y., Ed.; World Scientific: Singapore, 2000; Vol. 10B, p 1063f.
(5) Hotop, H.; Ruf, M.-W.; Allan, M.; Fabrikant, I. I. *Adv. At. Mol. Opt. Phys.* **2003**, *49*, 85.
(6) Modelli, A. *Trends in Chem. Phys.* **1997**, *6*, 57.
(7) Aflatooni, K.; Burrow, P. D. *J. Chem. Phys.* **2000**, *113*, 1455.
(8) Aflatooni, K.; Burrow, P. D. *Int. J. Mass Spectrom.* **2001**, *205*, 149.
(9) Gallup, G. A.; Aflatooni, K.; Burrow, P. D. *J. Chem. Phys.* **2003**, *118*, 2562.
(10) Burrow, P. D.; Modelli, A.; Chiu, N. S.; Jordan, K. D. *J. Chem. Phys.* **1982**, *77*, 2699.
(11) Underwood-Lemons, T.; Winkler, D. C.; Tossell, J. A.; Moore, J. H. *J. Chem. Phys.* **1994**, *100*, 9117.
(12) Orient, O. J.; Chutjian, A.; Crompton, R. W.; Cheung, B. *Phys. Rev. A* **1989**, *39*, 4494.
(13) Christophorou, L. G. *Z. Phys. Chem.* **1996**, *196*, 195.
(14) Andersen, T.; Haugen, H. K.; Hotop, H. *J. Phys. Chem. Ref. Data* **1999**, *28*, 1511.
(15) *Handbook of Chemistry and Physics*, 88th ed.; Lide, D. R., Ed.; CRC Press: Atlanta, GA, 2007−2008.
(16) Christophorou, L. G.; Olthoff, J. K.; Wang, Y. *J. Phys. Chem. Ref. Data* **1997**, *26*, 1205.
(17) Hahndorf, I.; Illenberger, E.; Lehr, L.; Manz, J. *Chem. Phys. Lett.* **1994**, *231*, 460.
(18) Wilde, R. S.; Gallup, G. A.; Fabrikant, I. I. *J. Phys. B* **1999**, *32*, 1.
(19) Fabrikant, I. I.; Hotop, H. *J. Chem. Phys.* **2008**, *128*, 124308.
(20) Smith, D.; Spaněl, P. *Adv. At. Mol. Opt. Phys.* **1994**, *32*, 307.
(21) Miller, T. M. *Adv. At. Mol. Opt. Phys.* **2005**, *51*, 299.
(22) Klar, D.; Ruf, M.-W.; Hotop, H. *Int. J. Mass Spectrom.* **2001**, *205*, 93.
(23) Braun, M.; Marienfeld, S.; Ruf, M.-W.; Hotop, H. *J. Phys. B* **2009**, *42*, 125202.
(24) Klar, D.; Ruf, M.-W.; Fabrikant, I. I.; Hotop, H. *J. Phys. B* **2001**, *34*, 3855.
(25) Global Aspects of Atmospheric Chemistry. In *Topics in Physical Chemistry*; Zellner, R., Ed.; Springer: Steinkopff, Darmstadt, 1999; Vol. 6.
(26) Jones, R. K. *J. Chem. Phys.* **1986**, *84*, 813.
(27) Field, D.; Jones, N. C.; Lunt, S. L.; Ziesel, J.-P.; Gulley, R. J. *J. Chem. Phys.* **2001**, *115*, 3045.
(28) Karwacz, P.; Brusa, R. S.; Zecca, A. *Riv. Nuovo Cimento Soc. Ital. Fis.* **2001**, *24* (4), 45–57.
(29) Yamada, T.; Ushiroda, S.; Kondo, Y. *J. Phys. B* **2008**, *41*, 235201.
(30) Mann, A.; Linder, F. *J. Phys. B* **1992**, *25*, 1633.
(31) Pejcev, V. M.; Kurepa, M. V.; Cadez, I. M. *Chem. Phys. Lett.* **1979**, *63*, 301.
(32) Illenberger, E.; Scheunemann, H.-U.; Baumgärtel, H. *Chem. Phys.* **1979**, *37*, 21.
(33) Illenberger, E. *Ber. Bunsen.-Ges. Phys. Chem.* **1982**, *86*, 252.
(34) Underwood-Lemons, T.; Gergel, T. J.; Moore, J. H. *J. Chem. Phys.* **1995**, *102*, 119.
(35) Kiendler, A.; Matejcik, S.; Skalny, J. D.; Stamatovic, A.; Märk, T. D. *J. Phys. B* **1996**, *29*, 6217.
(36) Denifl, G.; Muigg, D.; Walker, I.; Cicman, P.; Matejcik, S.; Skalny, J. D.; Stamatovic, A.; Märk, T. D. *Czech. J. Phys.* **1999**, *49*, 383.
(37) Langer, J.; Matt, S.; Meinke, M.; Tegeder, P.; Stamatovic, A.; Illenberger, E. *J. Chem. Phys.* **2000**, *113*, 11063.
(38) Matejcik, S.; Foltin, V.; Stano, M.; Skalny, J. D. *Int. J. Mass Spectrom,* **2003**, *223*−*224*, 9.
(39) Skalny, J. D.; Matejcik, S.; Mikoviny, T.; Märk, T. D. *Int. J. Mass Spectrom,* **2003**, *223*−*224*, 217.
(40) Claassen, H. H. *J. Chem. Phys.* **1954**, *22*, 50.
(41) Shimanouchi, T. *J. Phys. Chem. Ref. Data* **1974**, *3*, 269.
(42) Smith, D.; Adams, N. G.; Alge, E. *J. Phys. B* **1984**, *17*, 461.
(43) Burns, S. J.; Matthews, J. M.; McFadden, D. L. *J. Phys. Chem.* **1996**, *100*, 19436.
(44) LeGarrec, J. L.; Sidko, O.; Queffelec, J. L.; Hamon, S.; Mitchell, J. B. A.; Rowe, B. R. *J. Chem. Phys.* **1997**, *107*, 54.
(45) Wang, Y.; Christophorou, L. G.; Verbrugge, J. K. *J. Chem. Phys.* **1998**, *109*, 8304.
(46) Miller, T. M. Friedman, J. F. Schaffer, L. C. Viggiano, A. A. *J. Chem. Phys.*, in press.
(47) Chutjian, A.; Alajajian, S. H. *J. Phys. B* **1987**, *20*, 839.
(48) Hahndorf, I.; Illenberger, E. *Int. J. Mass Spectrom. Ion Proc.* **1997**, *167*−*168*, 87.
(49) Klar, D.; Ruf, M.-W.; Hotop, H. *Aust. J. Phys.* **1992**, *45*, 263.
(50) Klar, D.; Ruf, M.-W.; Hotop, H. *Meas. Sci. Technol.* **1994**, *5*, 1248.
(51) Weber, J. M.; Leber, E.; Ruf, M.-W.; Hotop, H. *Eur. Phys. J. D* **1999**, *7*, 587.
(52) Braun, M.; Barsotti, S.; Marienfeld, S.; Leber, E.; Weber, J. M.; Ruf, M.-W.; Hotop, H. *Eur. Phys. J. D* **2005**, *35*, 177.
(53) Wigner, E. P. *Phys. Rev.* **1948**, *73*, 1002.
(54) Field, T. A.; Slattery, A. E.; Adams, D. J.; Morrison, D. D. *J. Phys. B* **2005**, *38*, 255.
(55) Schramm, A.; Ruf, M.-W.; Stano, M.; Matejcik, S.; Fabrikant, I. I.; Hotop, H. *J. Phys. B* **2002**, *35*, 4179.
(56) Stepanović, M.; Pariat, Y.; Allan, M. *J. Chem. Phys.* **1999**, *110*, 11376.
(57) Fedor, J.; May, O.; Allan, M. *Phys. Rev. A* **2008**, *78*, 032701.
(58) May, O.; Fedor, J.; Allan, M. *Phys. Rev. A* **2009**, *80*, 012706.
(59) Kennerly, R. E. *Phys. Rev. A* **1980**, *21*, 1876.
(60) Fabrikant, I. I. *Phys. Rev. A* **1991**, *43*, 3478.
(61) Fabrikant, I. I.; Hotop, H.; Allan, M. *Phys. Rev. A* **2005**, *71*, 022712.
(62) Giorgianni, S.; Gambi, A.; Franco, L.; Ghersetti, S. *J. Mol. Spectrosc.* **1979**, *75*, 389.
(63) Kalin, S. A.; Kazansky, A. K. *J. Phys. B* **1990**, *23*, 4377.
(64) Kopyra, J.; Szamrej, I.; Graupner, K.; Graham, L. M.; Field, T. A.; Sulzer, P.; Denifl, S.; Märk, T. D.; Scheier, P.; Fabrikant, I. I.; Braun, M.; Ruf, M.-W.; Hotop, H. *Int. J. Mass Spectrom.* **2008**, *277*, 130.
(65) Rescigno, T. N.; Isaacs, W. A.; Orel, A.; Meyer, H.-D.; McCurdy, C. W. *Phys. Rev. A* **2002**, *65*, 032716.
(66) Graupner, K.; Graham, L. M.; Field, T. A.; Mayhew, C. A.; Fabrikant, I. I.; Miller, T. M.; Braun, M.; Ruf, M.-W.; Hotop, H. *Int. J. Mass Spectrom.* **2008**, *277*, 113.
(67) Mann, A. Private communication, 2009.